Inorganic Chemistry
Article

Inorg. Chem. **2009**, *48*, 10435–10441 **10435**
DOI: 10.1021/ic901559y

Effects of Ionic Liquids on the Characteristics of Synthesized Nano Fe(0) Particles

Yang Zhao,[†] Guirong Cui,[†] Jianji Wang,*[,†] and Maohong Fan[‡]

[†]*School of Chemical and Environmental Sciences, Henan Key Laboratory of Environmental Pollution Control, Henan Normal University, Xinxiang, Henan 453007, P. R. China, and* [‡]*School of Civil and Environmental Engineering, Georgia Institute of Technology, Atlanta, Georgia 30332*

Received August 5, 2009

In this paper, high specific surface area zerovalent Fe(0) nanoparticles with unusual morphology and high reductive activity were prepared using a chemical reductive reaction of iron chloride hydrate with sodium borohydride in an aqueous solution of ionic liquids (ILs). The ionic liquids, $[C_4mim]X$ ($X=Cl^-$, Br^-, BF_4^-, PF_6^-) and $[C_nmim][BF_4]$ (n=4, 6, 8), were used for this purpose. Transmission electron microscopy, X-ray diffraction, and Brunauer−Emmett−Teller surface area measurements were used to characterize the morphology, structure, and physical properties of the as-prepared Fe(0). The results suggest that the nucleation and growth of the Fe(0) were governed by an IL-controlled reductive reaction mechanism. The effects of ionic liquids (cations, anions, and concentration) on the morphology of the Fe(0) were examined. It was shown that anions of the ILs played a key role in the morphology and size of Fe(0), and the nanoparticle size of the Fe(0) prepared in the presence of different ionic liquids follows the trend: $[C_4mim]Cl > [C_4mim]Br > [C_4mim][BF_4] > [C_4mim][PF_6]$ and $[C_4mim][BF_4] > [C_6mim][BF_4] > [C_8mim][BF_4]$. The reductive activity of the iron nanoparticles was studied by the denitrification experiment of sodium nitrite. The removal rate of nitrite by the IL-capped Fe(0) was found to be much faster than that by the noncapped Fe(0). This indicates that the IL-capped Fe(0) particles are better candidates for the reductive degradation. The high reductive activity of the Fe(0) nanoparticles was attributed to their high surface area and more active sites.

Introduction

Iron nanoparticles have great potential for application in the fields of magnetic fluids,[1] catalysts for carbon nanotube formation,[2] magnetic resonance imaging contrast agents,[3,4] nickel−iron batteries, catalysts, and sorbents for environmental remediation.[5,6] Nanosized iron particles are effective for the transformation of a wide array of environmental contaminants such as chlorinated organic compounds,[7] toxic metals,[8,9] nitrate, and nitrite.[10−12]

A number of approaches have been developed to prepare iron nanoparticles. The two most common synthesis routes are the thermal decomposition[13−15] and the chemical reduction methods.[5,16−18] In the thermal decomposition method, iron pentacarbonyl ($Fe(CO)_5$) was dissolved in an organic solvent such as ether and then heated to about 200 °C. An organic surfactant such as oleic acid or decylamine was used to prevent the iron nanoparticles from aggregation. By this method, small and uniform iron nanoparticles can be prepared with high purity. However, this is not an economical process because high-temperature and highly expensive toxic precursors are needed. As a result, iron nanoparticles prepared by this route are not suitable for the applications where

*To whom correspondence should be addressed: E-mail: Jwang@henannu.edu.cn.

(1) Wu, K. T.; Yao, Y. D.; Wang, C. R.; Chen, P. F.; Yeh, E. T. *J. Appl. Phys.* **1999**, *85*, 5959.
(2) Wong, E. W.; Bronikowski, M. J.; Hoenk, M. E.; Kowalezyk, R. S.; Hunt, B. D. *Chem. Mater.* **2005**, *17*, 237.
(3) Jun, Y. W.; Huh, Y. M.; Choi, J. S.; Lee, J. H.; Song, H. T.; Kim, S.; Yoon, S.; Kin, K. S.; Shin, J. S.; Suh, J. S.; Cheon, J. *J. Am. Chem. Soc.* **2005**, *127*, 5732.
(4) Mornet, S.; Vasseur, S.; Grasset, F.; Duguet, E. *J. Chem. Mater.* **2004**, *14*, 2161.
(5) Tee, Y. H.; Grulke, E.; Bhattacharyya, D. *Ind. Eng. Chem. Res.* **2005**, *44*, 7062.
(6) Kanel, S. R.; Greneche, J. M.; Chol, H. *Environ. Sci. Technol.* **2006**, *40*, 2045.
(7) Wang, C.; Zhang, W. *Environ. Sci. Technol.* **1997**, *31*, 2154.
(8) Melitas, N.; Wang, J.; Conklin, M.; Farrell, J. *Environ. Sci. Technol.* **2002**, *36*, 2074.
(9) Li, X. Q.; Zhang, W. X. *J. Phys. Chem. C* **2007**, *111*, 6939.
(10) Devlin, J. F.; Eedy, R.; Butler, B. J. *J. Contam. Hydrol.* **2000**, *46*, 81.
(11) Miehr, R.; Tratnyek, M. M.; Bandstra, J. Z.; Scherer, M. M.; Alowitz, M. J. *Environ. Sci. Technol.* **2004**, *38*, 139.
(12) Su, C.; Puls, R. W. *Environ. Sci. Technol.* **2004**, *38*, 2715.
(13) Kim, D.; Park, J.; An, K. J.; Yang, N. K.; Park, J. G.; Hyeon, T. *J. Am. Chem. Soc.* **2007**, *129*, 5812.
(14) Farnell, D.; Majetich, S. A.; Wilcoxon, J. P. *J. Phys. Chem. B* **2003**, *107*, 11022.
(15) Kang, E.; Park, J.; Hwang, Y.; Kang, M.; Park, J. G.; Hyon, T. *J. Phys. Chem. B* **2004**, *108*, 13932.
(16) Glavee, G. N.; Klabunde, K. J.; Sorensen, C. M.; Hadjipanayis, G. C. *Inorg. Chem.* **1995**, *34*, 28.
(17) Guo, L.; Huang, Q. J.; Li, X. Y.; Yang, S. H. *Phys. Chem. Chem. Phys.* **2001**, *3*, 1661.
(18) Li, X. Q.; Zhang, W. X. *Langmuir* **2006**, *22*, 4638.

Published on Web 10/08/2009

large quantities of iron nanoparticles are required, such as environmental remediation.

Compared to the thermal decomposition method, the chemical reduction route is economical. In the chemical reduction process, an iron salt such as ferric chloride ($FeCl_3$) is reduced by sodium borohydride ($NaBH_4$) in aqueous solution to form iron nanoparticles. Unfortunately, the high air sensitivity is the main problem in the technological application of this material, and for that reason many different methods have been developed to prevent iron nanoparticles from oxidation and aggregation. Surfactants, polymers, quaternary ammonium salts, and polyoxoanions are often used as additives for the stabilization of transition-metal nanoparticles.[19−21]

Room temperature ionic liquids (ILs), which are generally composed of a bulky organic cation and a weakly coordinating anion, have attracted significant attention in many fields of chemistry and industry as environmentally benign solvents. ILs have many advantages, such as a low interface intension and high chemical and thermal stability. They can create an electrostatic protection layer for the transition-metal nanoparticles. Dupont et al.[22−26] and other researchers[27−29] have recently reported that imidazolium-based ionic liquids are an interesting medium for the formation and stabilization of catalytically active transition-metal nanoparticles such as Pt, Pd, Ir, Rh, Co, Au, and Ag. However, up to now, no studies have been reported for the creation of Fe(0) in ionic liquids, and the role of ILs played in the formation of nanoparticles is not clear.

In this work, iron nanoparticles were synthesized by a chemical reduction method from iron chloride hydrate ($FeCl_3 \cdot 6H_2O$) at mild temperature with sodium borohydride ($NaBH_4$) as the reducing agent. The imidazolium ionic liquids were used as both the control and the stabilization agents, including [C_4mim]X (X = Cl^-, Br^-, BF_4^-, PF_6^-) and [$C_n$mim][BF_4] (n = 4, 6, 8). The structure and properties of as-prepared products were characterized by means of X-ray diffraction (XRD), transmission electron microscopy (TEM), and Brunauer−Emmett−Teller (BET) surface area measurements. The reduction of sodium nitrite was chosen as a test reaction to prove the catalytic activity of iron nanoparticles. On the basis of various characterization techniques, the influences of ILs (cations, anions, and concentration) on the morphology and size were investigated in detail. The nanosized iron particles were found to have high reductive activity for sodium nitrite.

Experimental Section

Chemicals. The reagents used were 1-methylimidazole (99%, Shanghai Chem. Co.), 1-bromobutane (99%, Acros organic), 1-bromohexane (99%, Acros organic), 1-bromooctane (99%, Acros organic), 1-chlorobutane (99%, Acros organic), $FeCl_3 \cdot 6H_2O$ (A. R., Tianjin Chem. Co.), $NaBH_4$ (A. R., Shanghai Chem. Co.), N-(1-Naphthyl)ethylene diamine dihydrochloride (A.R., Beijing Chem. Co.), sodium nitrite (A. R., Beijing Chem. Co.), and sulfanilamide (A. R., Shanghai Chem. Co.). These chemical reagents were used as received.

Preparation of the ILs. [$C_n$mim]Br (n = 4, 6, 8) and [C_4mim]Cl were prepared and purified by using the procedure described in the literature.[30] Briefly, the reaction of 1-methylimidazole with excess 1-bromoalkane or 1-chlorobutane was preformed in 1,1,1-trichloroethane under reflux at 343 K for 48 h. The product [C_4mim]Br or [C_4mim]Br was recrystallized three times from ethyl acetate and ethyl acetate/acetonitrile (3:2 by volume) to remove any unreacted reagents. [C_6mim]Br and [C_8mim]Br were washed with 1,1,1-trichloroethane. The residual solvents were removed by heating at 70 °C under a vacuum. [$C_n$mim]-[BF_4] (n = 4, 6, 8) and [C_4mim][PF_6] were synthesized by adding dropwise the aqueous solution of sodium tetrafluoroborate or sodium hexafluorophosphate into the aqueous solution of [$C_n$mim]Br under vigorous stirring for 48 h. The resulting ionic liquids were extracted by dichloromethane, and deionized water was then added. The residual dichloromethane organic phases were removed from the product by rotary evaporation. All of the ionic liquids were dried under a vacuum at 70 °C for 2−3 days in the presence of P_2O_5. The composition and purity of the ILs were checked by ^{1}H NMR spectroscopy (Bruker, advance-400 MHz), and they were found to be in good agreement with those reported in the literature.[31]

Preparation of the Iron Nanoparticles. The preparation of iron nanoparticles was carried out by mixing solution A with solution B. Solution A was prepared by dissolving 1.35 g of $FeCl_3 \cdot 6H_2O$ into 40 mL of deionized water. Solution B was made by dissolving 0.95 g of $NaBH_4$ into 10 mL of deionized water. The deionized water was purged with highly pure argon for 2 h to remove oxygen before use. Solution A was placed in a three-necked round bottomed flask with an argon atmosphere at 30 °C. After 30 min of stirring with a magnetic stirrer, a light-yellow transparent solution was obtained. Solution B was then injected into solution A in less than 2 min using a 30 mL syringe under vigorous stirring. The reaction was as follows:

$$2FeCl_3 + 6NaBH_4 + 18H_2O \rightarrow 2Fe + 21H_2\uparrow + 6B(OH)_3 + 6NaCl \quad (1)$$

As the reaction proceeded, color of the solution changed from light-yellow to light-brown, accompanied by the appearance of gas bubbles. The solution turned to dark brown, and finally a black solution was obtained. Over an extended period of aging (1 h), the product particles were separated from the solution by centrifugation, washed with deionized water many times, and then washed with acetone at the end. Adding a few drops of acetone can remove the water quickly and hence lessen the reaction of iron with water and oxygen. The obtained product was dried at 60 °C under a vacuum for 6 h. In the investigation of IL effects, each of the ILs under study was added to solution A before it was mixed with solution B. The other reaction conditions were the same, and the procedures for the preparation of the iron particles mentioned above were followed.

(19) Guo, L.; Huang, Q. J.; Li, X. Y.; Yang, S. H. *Langmuir* **2006**, *22*, 7867–7872.
(20) Aiken, J. D.; Finke, R. G. *J. Am. Chem. Soc.* **1998**, *120*, 9545.
(21) Astruc, D.; Lu, F.; Aranzaes, J. R. *Angew. Chem., Int. Ed.* **2005**, *44*, 7852.
(22) Dupont, J.; Fonseca, G. S.; Umpierre, A. P.; Fichtner, P. F. P.; Teixeira, S. R. *J. Am. Chem. Soc.* **2002**, *124*, 4228.
(23) Scheeren, C. W.; Machado, G.; Dupont, J.; Fichtner, P. F. P.; Teixeira, S. R. *Inorg. Chem.* **2003**, *42*, 4738.
(24) Gelesky, M. A.; Umpierre, A. P.; Machado, G.; Correia, R. R. B.; Magno, W. C.; Morais, J.; Ebeling, G.; Dupont, J. *J. Am. Chem. Soc.* **2005**, *127*, 4588.
(25) Scheeren, C. W.; Machado, G.; Teixeira, S. R.; Morais, J.; Domingos, J. B.; Dupont, J. *J. Phys. Chem. B* **2006**, *110*, 13011.
(26) Migowski, P; Dupont, J. *Chem.—Eur. J.* **2007**, *13*, 32.
(27) Antonietti, M.; Kuang, D. B.; Smarsly, B.; Zhou, Y. *Angew. Chem., Int. Ed.* **2004**, *43*, 4988.
(28) Zhou, D.; Fei, Z.; Geldbach, T. J.; Scopelliti, R.; Dyson, P. J. *J. Am. Chem. Soc.* **2004**, *126*, 15876.
(29) Mu, X. D.; Meng, J. Q.; Li, Z. C.; Kou, Y. *J. Am. Chem. Soc.* **2005**, *127*, 9694.
(30) Dupone, J.; Consort, C. S.; Suarez, P. A. Z.; Souza, R. F. *Org. Synth.* **1999**, *79*, 236.
(31) Huddleston, J. G.; Visser, A. E.; Reichert, W. M.; Willaller, H. D.; Broker, G. A.; Roger, R. D. *Green Chem.* **2001**, *3*, 156.

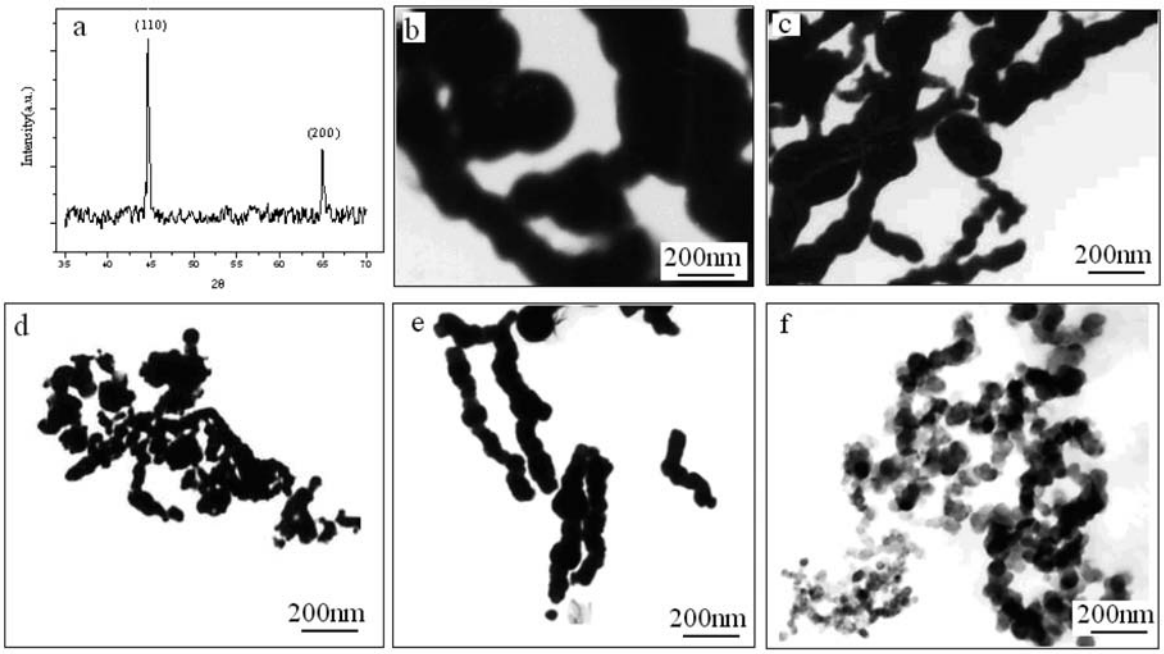

Figure 1. (a) X-ray diffraction pattern of Fe(0) nanoparticles prepared in the presence of $[C_4mim][PF_6]$ (w = 1:2). TEM images of Fe(0) nanoparticles prepared in the presence and absence of ILs: (b) in pure water, (c) in the presence of $[C_4mim]Cl$ (w = 1:5), (d) in the presence of $[C_4mim]Br$ (w = 1:5), (e) in the presence of $[C_4mim][BF_4]$ (w = 1:3), and (f) in the presence of $[C_4mim][PF_6]$ (w = 1:2).

Characterization of the Synthesized Iron Nanoparticles. The structures of the iron nanoparticles prepared in the presence of different ILs were characterized by XRD. The XRD experiments were carried out on a D8 X diffractometer (Germany, Bruker) with Cu Kα radiation (λ = 1.5406 Å). The scan data were collected in the 2θ range of 20−70°.

The morphology and particle size of the samples were determined by TEM on a JEM-100SX operating at accelerating voltages of 80 kV. A small amount of the sample was dispersed in a 95% ethanol solution which was purged with highly pure argon for 3 h to remove oxygen. After agitation under an ultrasonic environment for 2 h, one drop of the dispersed slurry was dipped onto a carbon-coated copper grid.

Specific surface areas of the synthesized iron nanoparticles were measured according to the BET method on a NOVA 1000e surface area and pore size analyzer.

Reductive Activity Estimation of the Iron Nanoparticles. The reductive activity of the obtained Fe(0) nanoparticles was estimated by the denitrification experiment of sodium nitrite. For this purpose, 0.060 g of the iron nanoparticles was added immediately to 100 mL of a sodium nitrite solution (10 mg N/L) under stirring at ambient temperature. The solution of sodium nitrite was deoxygenated by an argon stream for 2 h before the addition of Fe(0). At selected time intervals, the solution of a given volume was withdrawn with a syringe and then filtered with a 0.45 μm filter membrane. Then, the collected filtrates were immediately analyzed for their concentrations of nitrite and ammonium with a Shanghai 752 UV−vis spectrophotometer.[32−34] A control experiment was also performed with ILs only.

(32) *Water quality − Determination of nitrogen (nitrite) − Spectrophotometric method*, Standard GB 7493−87, State Environmental Protection Administration of China, **1987**.

(33) *Water quality − Determination of ammonium − Nessler's regent colorimetric method*, Standard GB 7497−87, State Environmental Protection Administration of China, **1987**.

(34) *Standard Methods for the Examination of Water and Wastewater*, 20th ed.; American Public Health Association: Washington, DC, **1998**.

Results and Discussion

XRD Studies. Figure 1a shows the XRD pattern of the iron nanoparticles prepared by the chemical reductive reaction between sodium borohydride and iron chloride at 30 °C in the presence of $[C_4mim][PF_6]$. It is evident that two broad diffraction peaks are observed at 44.6° and 65.1°, which are ascribable to the (110) and (200) planes, respectively. No characteristic peaks of impurities are found in Figure 1. All of the reflections of the XRD pattern can be indexed to pure body-centered cubic (bcc) α-Fe with unit cell parameter a = 2.8662 Å (JCPDS 87-0721). The mean diameter could be estimated from the XRD diffraction pattern by means of the Debye−Scherrer equation[35] calculated from the full width at half-maximum (fwhm) of the (110) and (200) planes. The Debye−Scherrer equation can be expressed by

$$D_{hkl} = 0.89\lambda/(\beta_{hkl} \cos \theta) \qquad (2)$$

where D_{hkl} is the crystallite size, λ is the wavelength of the incident ray, β_{hkl} is the full width at half-maximum of the peak, and θ is the position of plane peak. The average size of the iron nanoparticles is about 15 nm, calculated from the above equation. Similar XRD patterns have also been found for the iron particles prepared in the presence of the other studied ionic liquids.

Morphologies of the Iron Nanoparticles. TEM analysis provides further insight into the morphology and particle size of the iron nanoparticles. Figure 1b−f show the differences in the morphology and particle size of the samples under different preparation conditions. The sample, prepared with $FeCl_3$ in an aqueous medium without

(35) Klug, H.; Alexander, L. *X- ray Diffraction Procedures*; Wiley: New York, **1962**.

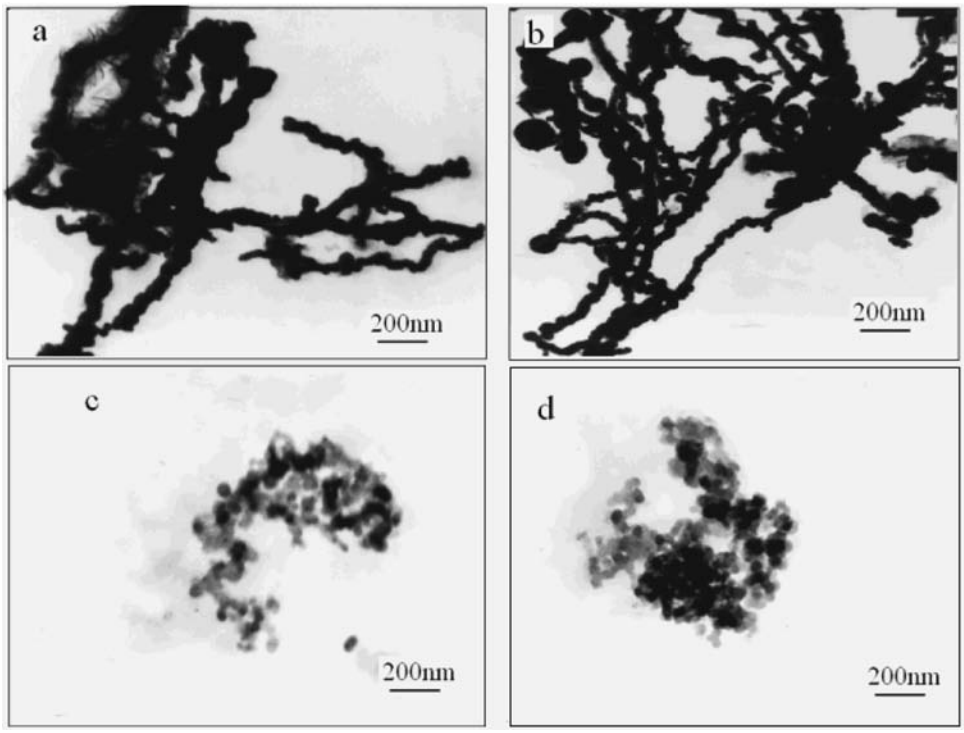

Figure 2. TEM images of Fe(0) nanoparticles prepared in the presence of $[C_4mim]^+$-based ILs: (a) $[C_4mim][BF_4]$ (w = 1:10), (b) $[C_4mim][BF_4]$ (w = 1:1), (c) $[C_4mim][PF_6]$ (w = 1:10), and (d) $[C_4mim][PF_6]$ (w = 1:1).

ILs, had an irregular chainlike aggregation morphology, as shown in Figure 1b. It can be seen that the irregular chainlike aggregates were composed of many small particles with 200−250 nm diameters and about 1 μm lengths.

In the presence of the ILs $[C_4mim]X$ (X = Cl^-, Br^-, BF_4^-, PF_6^-) in the $FeCl_3$ solution, it was found that the Fe(0) nanoparticle size became smaller and more uniform than that prepared in pure water. For the purpose of convenience, we defined w as the molar ratio of IL to $FeCl_3 \cdot 6H_2O$. As $[C_4mim]Cl$ (w = 1:5) or $[C_4mim]Br$ (w = 1:5) was present in the system, the morphology of the products was roughly spherical or chainlike, and the diameters and the average length of the chain decreased to 50 ± 12 nm and 600 ± 45 nm, respectively (see Figure 2c,d). When $[C_4mim][BF_4]$ (w = 1:3) was used, the morphology of Fe(0) shown in Figure 1e was similar to that prepared in the presence of $[C_4mim]Cl$ or $[C_4mim]Br$, but the size was more uniform, the diameter was smaller, and the chain of Fe(0) aggregates was very dispersive. A typical TEM image of the iron nanoparticles prepared in the presence of $[C_4mim][PF_6]$ (w = 1:2) was presented in Figure 1f. The iron nanoparticles were spherical, and the mean particle size was 20 ± 4 nm. The difference in the iron nanoparticles in Figure 1f and b−e was that the morphology of Fe(0) prepared in the presence of $[C_4mim][PF_6]$ was irregular chain aggregates formed by many single spheres. It can be seen from Figure 1b−f that the dispersibility of Fe(0) nanoparticles prepared in the presence of $[C_4mim][PF_6]$ was the best among the studied systems. From the comparison, it could be seen that the nature of anions of the ILs played an important role in affecting the morphology and size of Fe(0).

In order to examine the effect of the amount of ILs added, different molar ratios of $[C_4mim][BF_4]$ or $[C_4mim][PF_6]$ to $FeCl_3 \cdot 6H_2O$ were chosen for the study. When the molar ratio of $[C_4mim][BF_4]$ to $FeCl_3 \cdot 6H_2O$ was w = 1:10, but keeping other reaction conditions unchanged, a spherical chainlike Fe(0) was obtained, as proven by the TEM image shown in Figure 2a. The spheres were not uniform, and the chains were crossed together. As the amount of $[C_4mim][BF_4]$ was increased to w = 1:9, 1:7, 1:5, and 1:4, the morphology of Fe(0) was similar to that at w = 1:10 (not shown). If the w value was changed to 1:3, the morphology of Fe(0) was chainlike aggregates formed by small and uniformed spheres, as shown in Figure 1e. The uniformity of the size was better than that prepared in the presence of $[C_4mim][BF_4]$ (w = 1:10). When the amount of $[C_4mim][BF_4]$ was further increased to 1:1, the nanoparticles of Fe(0) aggregated into chains, as shown in Figure 2b. It can be seen that they were severe conglobulations. Therefore, the best amount of $[C_4mim][BF_4]$ should be w = 1:3. When $[C_4mim][BF_4]$ was replaced by $[C_4mim][PF_6]$, different sized nanospheres could be obtained by changing the w value. Figures 1f and 2c,d show images of Fe(0) prepared in the presence of $[C_4mim][PF_6]$ (w = 1:2, 1:10, and 1:1, respectively). In the case of w = 1:10, slightly gathered irregular nanospheres were obtained, and their diameter was about 50 ± 8 nm. The size of Fe(0) increased with the increase of the w value. When the w value was increased to 1:2, a small-sized (about 20 nm) and uniform nanosphere was obtained, as shown in Figure 1f. As the w value was further increased to 1:1, the morphology of Fe(0) was similar to that at w = 1:10, and the irregular nanospheres gathered severely. On the basis of the above comparison, it is clear that the amount of $[C_4mim][PF_6]$ at w = 1:2 is

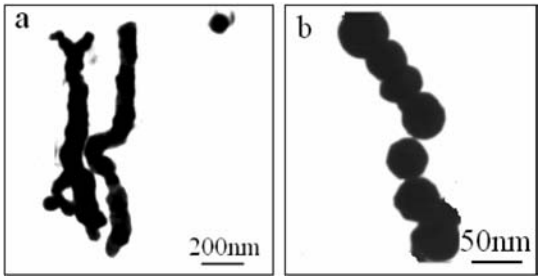

Figure 3. TEM images of iron nanoparticles prepared in the presence of $[BF_4]^-$-based ILs: (a) $[C_6mim][BF_4]$, (b) $[C_8mim][BF_4]$.

required for the preparation of the small sized and uniformed nanosphere. At the same time, the best amount of $[C_4mim]Cl$ (w = 1:5) and $[C_4mim]Br$ (w = 1:5) can also be obtained

To investigate the influence of the alkyl chain length of the ILs, $[C_nmim][BF_4]$ (n = 4, 6, 8; w = 1:3) was chosen as an additive to fabricate the Fe(0) nanomaterials. Figure 3a shows a typical TEM image of the iron nanoparticles prepared in the presence of $[C_6mim][BF_4]$. The particle morphology was similar to that prepared in the presence of $[C_4mim][BF_4]$ (see Figure 1e), but the sphere of the chain was more uniform and the size was smaller in the presence of $[C_6mim][BF_4]$. Figure 3b gives the TEM image of the Fe(0) nanoparticles resulting from the addition of $[C_8mim][BF_4]$, which demonstrated that the nanoparticle was spherical and three or four nanospheres were organized into chainlike aggregates. The size of the sphere was 20 ± 3 nm, and the size distribution was narrow. From the comparison between Figures 1e and 3, it can be found that the size of the Fe(0) nanoparticle decreased with the alkyl chain length in the order $[C_4mim][BF_4] > [C_6mim][BF_4] > [C_8mim][BF_4]$.

The Possible Formation Mechanism. In the investigation of the formation mechanism, whether the ILs were trapped on the surface of Fe(0) or not was studied first by UV−vis spectroscopy, and the Fe(0) prepared in the presence of $[C_4mim][PF_6]$ was selected as an example. The measurements were performed at the maximum absorption wavelength (211 nm) of $[C_4mim][PF_6]$ in water.[36] It was found that the $[C_4mim][PF_6]$ concentration was 5.28×10^{-5} mol/L in the Fe(0) samples. From this result, it can be concluded that small amounts of the ILs were trapped on the surface of Fe(0). On the other hand, the Fe(0) nanoparticles prepared in the presence of ionic liquids were very stable, and they could not be broken into discrete spheres even under ultrasonication for 5 h. This suggested that the chainlike aggregates were not formed through magnetism attraction. As a result, one possible reductive mechanism controlled by ionic liquids was proposed, as shown in Figure 4. When there was no ionic liquid present in the reaction solution, the Fe^{3+} reacted quickly with $NaBH_4$ to form small Fe(0) nanoparticles, which were aggregated into a long chain via magnetism attraction. As the ionic liquid $[C_nmim]X$ was present in the solution, the Fe^{3+} was surrounded by anions of the ILs through the electrostatic interaction, and the cation of the ILs was outside the anion. Thus, the polymeric superstructure would be formed by hydrogen

(36) Zhou, Y.; Schattka, J. H.; Antonietti, M. *Nano Lett.* **2004**, *4*, 477.

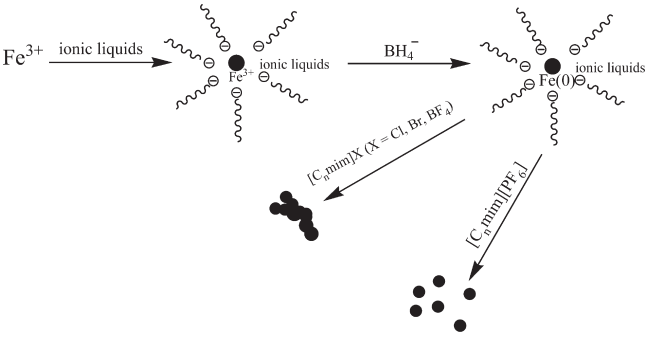

Figure 4. A schematic illustration for the reductive mechanism controlled by ionic liquids: (⊖) anion of ILs, (〰) cation of ILs, and (●) Fe^{3+} and Fe(0).

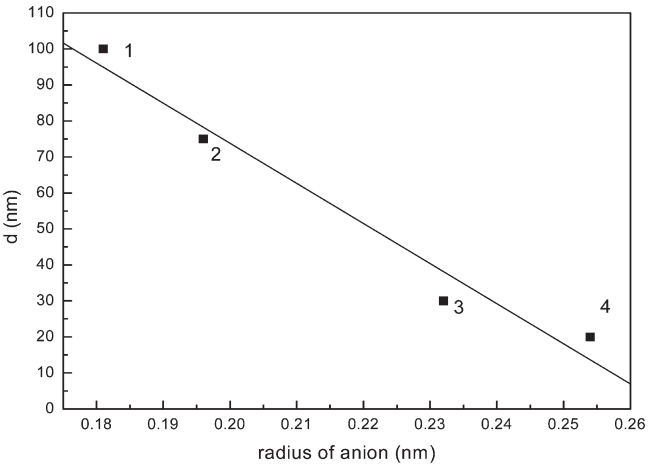

Figure 5. The linear relationship between the size of the Fe(0) nanoparticles and the radius of the ILs anions: 1, Cl^-; 2, Br^-; 3, BF_4^-; 4, PF_6^-.

bonds or other noncovalent interactions between cations and anions of the ILs. Under these circumstance, the newly formed Fe(0) from the reaction between Fe^{3+} and $NaBH_4$ was coated by the polymeric superstructure of ILs, which would prevent iron nanoparticles from aggregation. Thus, the Fe(0) nanoparticle was uniform, and its size was small. Actually, a reasonable linear relationship was observed between the size of the Fe(0) particles and the radius of the ILs anions, as shown in Figure 5. This indicated that anions of the ILs played a key role in the morphology of nanoparticles, and more perfect nanoparticles were formed in the presence of the ILs with a larger sized anion (PF_6^-) compared to those ILs with smaller sized anions (Cl^-, Br^-, or BF_4^-).

In addition to anions of the ILs, the cations also influenced the morphology and size of Fe(0). As mentioned above, the well-organized chainlike iron can be fabricated in the presence of $[C_8mim][BF_4]$. The main effect of the alkyl chain length on morphology was the steric barrier, which increased with the length of the alkyl chains. Therefore, as the alkyl chain length of the ILs cations increased, the aggregation of iron nanoparticles became difficult, and then the size of the particles was small.

Reductive Activity of the Iron Nanoparticles. The nitrite solutions with (pH = 3.0, 5.0) and without pH control have been used to investigate the effect of the initial pH of the solutions on nitrite reduction by iron nanoparticles.

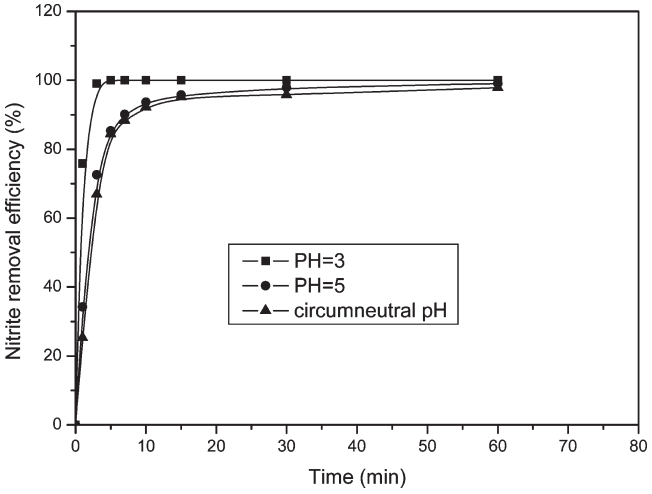

Figure 6. The time dependence of nitrite removal efficiency by Fe(0) nanoparticles prepared in the presence of $[C_4mim][BF_4]$ under different pH's. Initial nitrite concentration was 10 mg N L^{-1}, and the initial dosage of Fe(0) was 0.6 g L^{-1}.

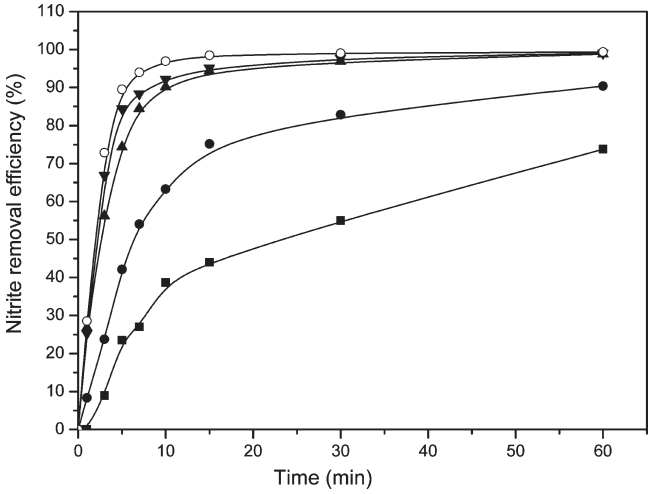

Figure 7. The time dependence of nitrite removal efficiency by Fe(0) nanoparticles prepared in the presence of ILs without pH control: (●) $[C_4mim]Cl$, (▲) $[C_4mim]Br$, (▼) $[C_4mim][BF_4]$, (○) $[C_4mim][PF_6]$, or (■) H_2O. Initial dosage of Fe(0) was 0.6 g·L^{-1}, and initial nitrite concentration was 10 mg N L^{-1}.

The result is shown in Figure 6 where the Fe(0) nanoparticle prepared in the presence of $[C_4mim][BF_4]$ is used as an example. It can be seen that the initial pH of the solutions does not appear to have a strong effect on the nitrite reduction rate. When no pH control was provided, nitrite was completely removed after a reaction time of 30 min. This is the same as in the systems with pH control. This result suggests that the application of this degradation technique dose not require a harsh low-pH environment and allows a wider range of pH. A similar trend was also found in the nitrite reduction using the Fe(0) nanoparticle prepared in the presence of other ILs. Therefore, the system without pH control was used in the following investigation.

The reductive activity of the Fe(0) nanoparticles prepared in pure water and in aqueous $[C_4mim]X$ ($X = Cl^-$, Br^-, BF_4^-, PF_6^-) ionic liquids was examined with a denitrification experiment using sodium nitrite. The variation of nitrite concentration with time is shown in Figure 7. It can be seen that the removal efficiency of nitrite by the IL-capped Fe(0) is about 4 times that by the noncapped Fe(0) after a reaction time of 5 min. This verifies that the IL-capped Fe(0) particles are much better candidates for reductive degradation. The ionic liquids in aqueous solutions affect the reductive activity of the Fe(0) in the order $[C_4mim][PF_6] > [C_4mim][BF_4] > [C_4mim]Br > [C_4mim]Cl$.

The controlled degradation experiment was also conducted in the absence of Fe(0) nanoparticles (i.e., ILs only). The result revealed that no change in the concentration of nitrite was detected for a period of 3 h. This suggests that ILs have no effect on the degradation of nitrite. According to this result, the effect of the anion of the ILs on the degradation can be explained by the specific surface areas of Fe(0) nanoparticles prepared in the presence of ILs. The specific surface areas of 148.73, 116.81, 59.59, and 29.69 $m^2\ g^{-1}$ have been determined for Fe(0) nanoparticles prepared, respectively, in the presence of $[C_4mim][PF_6]$, $[C_4mim][BF_4]$, $[C_4mim]Cl$, and H_2O. No such high specific surface areas have been reported in the literature for Fe(0) nanoparticles.[37] From

(37) Wang, W.; Jin, Zh; Li, T. L.; Zhang, H.; Gao, S. *Chemosphere* **2006**, *65*, 1396.

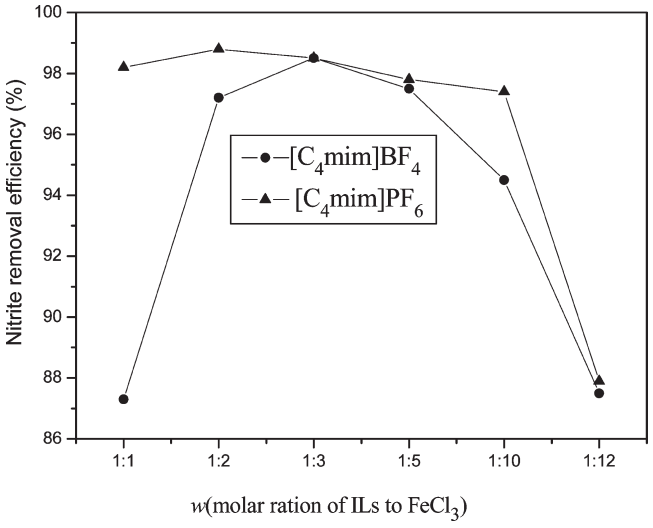

Figure 8. The reductive activity of Fe(0) under different molar ratios of $[C_4mim][BF_4]$ to $FeCl_3 \cdot 6H_2O$ or $[C_4mim][PF_6]$ to $FeCl_3 \cdot 6H_2O$ without pH control. Initial dosage of Fe(0) was 0.6 g L^{-1}, and initial nitrite concentration was 10 mg N L^{-1}.

a comparison of the specific surface areas, it was found that Fe(0) nanoparticles with higher specific surface areas displayed higher reductive activity.

The reductive activity of Fe(0) nanoparticles prepared in the presence of different amounts of $[C_4mim][BF_4]$ or $[C_4mim][PF_6]$ was also examined. Figure 8 shows the curves of the removal efficiency of sodium nitrite versus the molar ratios (w) of the ILs to $FeCl_3$. It can be seen that the reductive activity increases initially then decreases with the decrease of w values. The results suggest that the reductive activity of Fe(0) is the highest in the presence of $[C_4mim][BF_4]$ (w = 1:3) or $[C_4mim][PF_6]$ (w = 1:2). These results indicate that the preparation conditions significantly affect the surface areas of Fe(0) nanoparticles, thus enhancing their catalytic activity.

The formation of NH_4^+ or N_2 as the final product has been examined. Analytical data demonstrated that

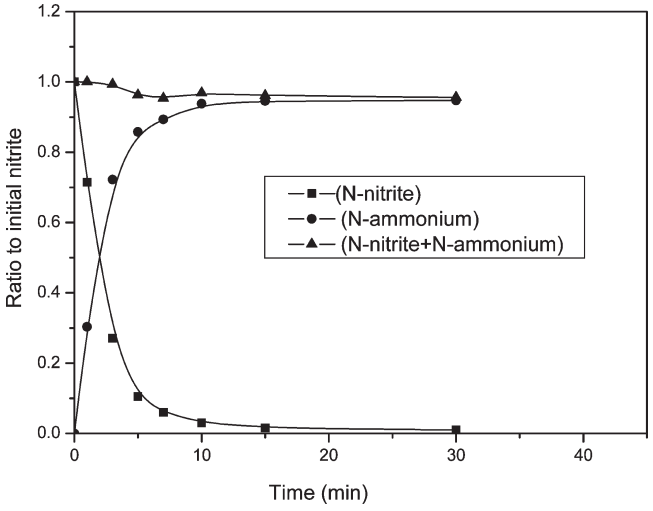

Figure 9. Nitrogen mass balance of the sum of nitrite and ammonium under the condition without pH control. Fe(0) nanoparticles were prepared in the presence of $[C_4mim][PF_6]$, initial dosage of Fe(0) was 0.6 g L^{-1}, and initial nitrite concentration was 10 mg N L^{-1}.

ammonium was the major final product of nitrite reduction. Figure 9 shows the results by using the Fe(0) nanoparticles prepared in the presence of $[C_4mim][PF_6]$ as an example; the other iron nanoparticles have similar trends. It can be seen from Figure 9 that N-ammonium accounts for more than 90% of the total converted N-nitrite. The slight difference between the initial concentration of N-nitrite and the sum of the concentrations of remaining N-nitrite and N-ammonium might be due to the generation of a small unmeasured amount of nitrogen gas through the reaction.

Conclusions

High specific surface area Fe(0) nanoparticles with spherical or chainlike aggregates were prepared, for the first time, using a reduction reaction of iron chloride hydrate with sodium borohydride in aqueous ILs $[C_4mim]X$ ($X = Cl^-$, Br^-, BF_4^-, PF_6^-) or $[C_nmim][BF_4]$ (n = 4, 6, 8). X-ray diffraction results indicated that the iron nanoparticles were composed of bcc α-Fe. An investigation of the effect of the ILs (anion, cation, and the concentration) on the morphology of the Fe(0) indicated that the anions of the IL played a key role in the morphology and size of Fe(0), and the nanoparticle size prepared in the presence of different ionic liquids follows the trend: $[C_4mim]Cl$ > $[C_4mim]Br$ > $[C_4mim][BF_4]$ > $[C_4mim][PF_6]$ and $[C_4mim][BF_4]$ > $[C_6mim][BF_4]$ > $[C_8mim][BF_4]$. It is suggested that there was an ionic liquid protective layer surrounding the nanoparticle surface, which prevented the nanoparticles from aggregating. Thus, a possible reductive mechanism controlled by ionic liquids was proposed. Moreover, a denitrification reaction of sodium nitrite was used to test the reductive activity of the Fe(0) at ambient temperature under conditions without pH control. It was found that the Fe(0) prepared in the presence of $[C_4mim][PF_6]$ showed the highest activity due to both the highest surface areas and more active sites. It is expected that the synthesis route described in the present work can be used to fabricate more other transition-metal nanoparticles.

Acknowledgment. This work was supported financially by the National Natural Science Foundation of China (No.20873036, 20573034) and the Program for Science & Technology Innovation Talents in Universities of Henan Province (No.2009HASTIT005). The authors gratefully acknowledge the reviewers for their valuable suggestions.